About the Lode angle infuence in ductile fracture

Carlos Felipe Guzmán*
Department ArGEnCo, Université de Liège, Belgium

October 6, 2013

Contents

*cf.guzman@ulg.ac.be

1 Introduction

Ductile fracture is a local phenomenon and the state of stress and strain in potential fracture locations should be determined [Bai and Wierzbicki, 2008]. In particular, it is known that the stress state affects the growth rate of cavities (See Lassance et al. [2007] for further references). When the stress triaxiality is not enough to describe the stress state, we can use the Lode parameter [Zhang et al., 2001]. Originally proposed by Lode [1926], this parameter includes the second and third invariant of the deviatoric stress tensor. In this report a state of the art is presented showing the influence of this parameter into micro/macro mechanical models and damage development. Different definitions of the Lode angle exists depending on the author, and they are also presented.

2 Lode angle definition

As using a stress tensor to characterise a stress state could be cumbersome, researchers usually use simpler dimensionless scalar metrics in order to represent a particular stress state. Between them we found the triaxiality and the Lode [1926] parameter. In this section, we define the Lode angle both in the stress invariants sense and as a vector in the stress space. *Einstein tensor notation* is used hereafter.

2.1 Stress invariants

Given the characteristic polynomial of σ_{ij}:

$$\lambda_{1,2,3}{}^3 - I_1\lambda_{1,2,3}{}^2 + I_2\lambda_{1,2,3} - I_3 = 0 \tag{1}$$

Where $\lambda_{1,2,3}$ is a Lagrange multiplier (principal stresses) and $I_{1,2,3}$ are the invariants of the stress tensor, defined as:

$$I_1 = \mathrm{tr}\sigma_{ij} = \sigma_{xx} + \sigma_{yy} + \sigma_{zz} \tag{2}$$

$$I_2 = \frac{1}{2}\sigma_{ij}\sigma_{ij} = \sigma_{xx}\sigma_{yy} + \sigma_{xx}\sigma_{zz} + \sigma_{yy}\sigma_{zz} - \sigma_{xy}{}^2 - \sigma_{xz}{}^2 - \sigma_{yz}{}^2 \tag{3}$$

$$I_3 = \det\sigma_{ij} \tag{4}$$

In terms of the principal stresses:

$$I_1 = \sigma_1 + \sigma_2 + \sigma_3 \tag{5}$$

$$I_2 = \sigma_1\sigma_2 + \sigma_2\sigma_3 + \sigma_1\sigma_3 \tag{6}$$

$$I_3 = \sigma_1\sigma_2\sigma_3 \tag{7}$$

The *hydrostatic* (aka mean) stress is defined by:

$$\sigma_h = \frac{1}{3} I_1 \tag{8}$$

So the *deviatoric* part of the stress tensor is:

$$\sigma_{ij} = s_{ij} + \sigma_h \delta_{ij} \tag{9}$$

The deviatoric stress invariants are:

$$J_1 = \mathrm{tr} s_{ij} = 0 \tag{10}$$

$$J_2 = \frac{1}{2} s_{ij} s_{ij} = -s_{xx}s_{yy} - s_{xx}s_{zz} - s_{yy}s_{zz} \tag{11}$$

$$= \frac{1}{6}[(\sigma_{xx} - \sigma_{yy})^2 + (\sigma_{yy} - \sigma_{zz})^2 + (\sigma_{zz} - \sigma_{xx})^2] +$$

$$+ {\sigma_{xy}}^2 + {\sigma_{yz}}^2 + {\sigma_{xz}}^2 = \frac{1}{3}\left(I_1^2 - 3I_2\right) \tag{12}$$

$$J_3 = \det s_{ij} = \frac{1}{27}\left(2I_1^3 - 9I_1 I_2 + 27 I_3\right) \tag{13}$$

The relation between the second deviatoric stress invariant and the von Mises equivalent stress is:

$$J_2 = \frac{1}{3}\sigma_{eq}^2 \tag{14}$$

Triaxiality is defined as:

$$T = \frac{\sigma_h}{\sigma_{eq}} = \frac{1}{3\sqrt{3}} \frac{I_1}{\sqrt{J_2}} \tag{15}$$

2.2 In the stress space

Usually, a stress state in the π-plane is represented through the principal stress $\sigma_{1,2,3}$ (the *Haigh-Westergaard* space). But is also possible to represent through the stress invariants. Equivalently, for a yield criterion initially isotropic, the dependence of the yield function f is on the stress invariants or the deviatoric stress invariants $J_{2,3}$. Moreover, any stress state in the *Haigh-Westergaard* space can be represented with a position vector $\overrightarrow{OP}$, which can be decomposed into:

$$\overrightarrow{OP} = \underbrace{\overrightarrow{ON}}_{\text{Hydrostatic}} + \underbrace{\overrightarrow{NP}}_{\text{Deviatoric}} \tag{16}$$

Where $\overrightarrow{ON} \perp \overrightarrow{NP}$ and $\overrightarrow{NP}$ lies on the π-plane. So, a curve in the π-plane can also be represented through polar coordinates related to the vector $\overrightarrow{NP}$ for mean-stress independent yield functions, or in terms of the magnitude and the orientation of this vector. It can be shown that the magnitude of this vector is $\sqrt{2J_2}$, and the orientation with respect to the deviatoric plane is called *Lode angle*, ξ_{Lode}. That is:

$$\|\overrightarrow{NP}\|_2 = \|\boldsymbol{S}\|_2 = \sqrt{\boldsymbol{S} : \boldsymbol{S}} = \sqrt{2J_2} \tag{17}$$

As the Lode angle is defined between one axis and the $\overrightarrow{NP}$ vector, it is necessary to get the projection of this vector respect to a determined axis of the principal stresses. For convenience, the following definition is taken respect to the projection of the first principal stress (with $\sigma_1 > \sigma_2 > \sigma_3$). This leads to [Khan and Huang, 1995, Voyiadjis et al., 2012]:

$$\cos 3\xi_{Lode} = \frac{3\sqrt{3}}{2}\frac{J_3}{J_2^{\frac{3}{2}}} \qquad 0^\circ \leq \xi_{Lode} \leq 60^\circ \tag{18}$$

Where ξ_{Lode} is the Lode angle in degrees. So, any stress state could be represented for the next equation [Khan and Huang, 1995]:

$$\begin{pmatrix} \sigma_1 \\ \sigma_2 \\ \sigma_3 \end{pmatrix} = \frac{I_1}{3}\begin{pmatrix} 1 \\ 1 \\ 1 \end{pmatrix} + \frac{2}{\sqrt{3}}\sqrt{J_2}\begin{pmatrix} \cos\xi_{Lode} \\ \cos\left(120 - \xi_{Lode}\right) \\ \cos\left(120 + \xi_{Lode}\right) \end{pmatrix} \tag{19}$$

Eq. 19 can also be written in terms of the equivalent von Mises stress and the triaxiality [Danas and Ponte Castañeda, 2012][1]:

$$\frac{3}{2\sigma_{eq}}\begin{pmatrix} \sigma_1 \\ \sigma_2 \\ \sigma_3 \end{pmatrix} = \frac{3}{2}T\begin{pmatrix} 1 \\ 1 \\ 1 \end{pmatrix} + \frac{2}{\sqrt{3}}\sqrt{J_2}\begin{pmatrix} -\cos\left(\xi_{Lode} + 60\right) \\ -\cos\left(\xi_{Lode} - 60\right) \\ \cos\xi_{Lode} \end{pmatrix} \tag{20}$$

The stress components of the left side of the equation are called *normalized principal stress components*.

2.3 Stress states

It is easy to see from Eq. 19 and 20 that different stress states can be obtained from different values of the Lode angle. For instance, for Eq. 19:

- $\xi_{Lode} = 0$: uniaxial tension plus hydrostatic pressure (triaxial tension).
- $\xi_{Lode} = 30$: pure shear plus hydrostatic pressure.
- $\xi_{Lode} = 60$: uniaxial compression plus hydrostatic pressure.

[1] Note the slightly difference in the principal directions, using $\sigma_3 > \sigma_1 > \sigma_2$ instead.

2.4 Other definitions

In terms of the principal stresses space, the *Lode's parameter* is defined as:

$$\mu_\sigma = \frac{2\sigma_2 - \sigma_1 - \sigma_3}{\sigma_1 - \sigma_3} \qquad -1 \leq \mu \leq 1 \tag{21}$$

With $\sigma_1 > \sigma_2 > \sigma_3$. This was the original proposal by Lode [1926], and is usually used in Civil engineer [Zhang et al., 2001]. The relation between the Lode parameter and the Lode angle of Eq.18 is given by:

$$\mu_\sigma = -\sqrt{3}\tan\xi_{Lode} \tag{22}$$

Other authors [Wierzbicki et al., 2005, Coppola et al., 2009, Gao et al., 2009, Danas and Ponte Castañeda, 2012] prefer to use the parameter:

$$X = \cos 3\xi_{Lode} = \pm\frac{27}{2}\frac{J_3}{\sigma_{eq}^3} \qquad -1 \leq X \leq 1 \tag{23}$$

Which is the same as Eq.18 using Eq.14. The $\pm$ sign depends on the author. Dunand and Mohr [2011a] called parameter X as the *normalized third invariant*. Danas and Ponte Castañeda [2012] also used Eq.23 but multiply by -1. Li et al. [2011] in Eq. 4 wrongly define X using σ_h instead of σ_{eq}. Other modification was introduced by Bai and Wierzbicki [2008] and used by Bai and Wierzbicki [2009], Dunand and Mohr [2011a], Malcher et al. [2012], Beese and Mohr [2012]:

$$\overline{\theta} = 1 - \frac{6\xi_{Lode}}{\pi} = 1 - \frac{2}{\pi}\arccos X \qquad -1 \leq \overline{\theta} \leq 1 \tag{24}$$

Which was called *normalized Lode angle*. Nahshon and Hutchinson [2008] slightly modified the Eq.23 to be in the positive range, in order to include it into their shear modified version of the GTN model:

$$\omega = 1 - X^2 = 1 - \left(\frac{27}{2}\frac{J_3}{\sigma_{eq}}\right)^2 \qquad 0 \leq \omega \leq 1 \tag{25}$$

With $\omega = 0$ for all axisymmetric stress states and $\omega = 1$ for pure shear plus a hydrostatic contribution. Voyiadjis et al. [2012] proposed:

$$\overline{\theta}_V = \sin 3\xi_{Lode} = \sqrt{1 - \frac{27}{4}\frac{J_3^2}{J_2^3}} \qquad 0 \leq \overline{\theta}_V \leq 1 \tag{26}$$

Which is obtained by applying a Pythagorean identity to Eq.18.

A totally different approach, based on strain and not stress, is presented by Morgeneyer and Besson [2011].

$$\mu_{\dot{p}} = \frac{\dot{p}_2}{\dot{p}_1 - \dot{p}_3} \tag{27}$$

Where $\dot{p}_1$ are the principal values of the plastic strain tensor.

The Table 1 shows the different definitions presented here and their references.

Table 1: Table resuming the Lode angle defintions found in the literature.

Definition	Range	Reference	Name
$\mu_\sigma = \frac{2\sigma_2 - \sigma_1 - \sigma_3}{\sigma_1 - \sigma_3}$	$-1 \leq \mu_\sigma \leq 1$	Lode [1926]	Lode parameter
$\cos 3\xi_{Lode} = \frac{3\sqrt{3}}{2} \frac{J_3}{J_2^{\frac{3}{2}}}$	$0^\circ \leq \xi \leq 60^\circ$		Lode angle
$X = \frac{27}{2} \frac{J_3}{\sigma_{eq}^3}$	$-1 \leq X \leq 1$	Wierzbicki et al. [2005]	Normalized third invariant
$\overline{\theta} = 1 - \frac{2}{\pi} \arccos X$	$-1 \leq \overline{\theta} \leq 1$	Bai and Wierzbicki [2008]	Normalized Lode angle
$\omega = 1 - X^2$	$0 \leq \omega \leq 1$	Nahshon and Hutchinson [2008]	
$\overline{\theta}_V = \sqrt{1 - \frac{27}{4} \frac{J_3^2}{J_2^3}}$	$0 \leq \overline{\theta}_V \leq 1$	Voyiadjis et al. [2012]	
$\mu_{\dot{p}} = \frac{\dot{p}_2}{\dot{p}_1 - \dot{p}_3}$		Morgeneyer and Besson [2011]	Lode parameter for strain rates

3 State of the art

3.1 Motivations

The effect of the stress invariants on mechanical behaviour of materials dates back with the first J_2-plasticity models developed in the early 20th century to describe yielding of metals. The mean stress was later included to describe porous media subjected to hydrostatic pressure [Drucker and Prager, 1952]. Nevertheless, the study of the third invariant of the deviatoric stress is quite recent and it was mainly used in the frame of civil engineering. For instance, Bardet [1990] studied the influence of the Lode angle over the yield surface of pressure insensitive materials.

The approach for ductile fracture has follow a different way. The effect of the mean stress in damage development and fracture is very well established and numerous studies exist. Nevertheless, the importance of this parameter resurfaced when studying phenomenas involving low triaxialities levels[2], such as metal forming processes. Besides, some researchers have included these invariants into more general modified plasticity models to predict localization [Brünig et al., 2000] and fracture [Bai and Wierzbicki, 2008]. The inherent complexity of damage phenomena makes difficult, even for a simple tensile test, to distinguish between the softening induced by suppression of the dislocation motion and the softening due to porosity (*Gurson type* of softening) [Bai and Wierzbicki, 2008]. In the following review, the effect of the Lode angle on plastic yield is not reviewed, and damage and fracture are considered to be mainly dependent on the nucleation, growth and coalescence of voids.

Since his formulation, the Gurson [1977] model and the Tvergaard and Needleman [1984] (GTN) extension assumes that the voids are spherical during the deformation. Furthermore, the model only includes the triaxiality as the parameter describing the stress state. As mentioned by Pardoen [2006], this historical framework maybe came from the analysis of *crack-tip* problems, which are characterized by large stress triaxiality, in which shape effects are usually not important. Nevertheless, one of the limitations of using only triaxiality and spherical voids became apparent when Gologanu et al. [1996] observed that the void expansion can vary in different directions under the same triaxiality. Following this point, Zhang et al. [2001] made a 3D numerical analysis of a spherical void to look for the influence of the Lode parameter into the directional expansion of the void. He considered symmetry of a cubic cell, where the displacements at the boundaries were calculated from a given value of triaxiality and the Lode parameter. It was observed that both the deformation pattern of the void and the void volume fraction are influenced by the Lode parameter. Another interesting observation is that the influence of the Lode parameter seems to diminish with increasing triaxiality.

3.2 Developments

Dealing with low values of triaxiality stress states could be problematic in the Gurson model. In some cases, like in shear-dominated deformations, triaxiality is near zero or even negative [Nahshon and Hutchinson, 2008]

[2]Usually, low triaxiality means values under $\frac{1}{3}$.

predicting almost no increase of damage (voids do not grow under pure shear). Pardoen [2006] study the effect of the void shape at low triaxiality, mentioning that the void elongates in the direction of maximum strain. By using a modified version of the Gurson model, which considers growth, coalescence of *spheroidal*[3] voids and aspect radio of voids[4], it is confirmed that shape effects and coalescence are significant, as in Fig. 2.

Barsoum and Faleskog [2007a,b] analized the rupture mechanism of a mid and high strength steel in double notched axisymmetric specimens, subjected to combined tension and torsion. They found that when triaxiality is high, the specimens fail by *internal necking*, while for low triaxiality is due to *plastic shear localization* (aka *shear bands*). These two coalescense mechanisms were previously described by Pardoen and Brechet [2004] and Bron and Besson [2006] and they are showed in Fig. 3. At medium levels of triaxiality, this mechanisms may co-operte or even compete.

Barsoum and Faleskog [2007a] performed a micromechanical study of an array of cells to investigate the transition between these two mechanisms. By using this approach, the array of voids can be seen as an initial imperfection inducing internal necking, shear localization or both, as in Fig. 4. The strain localization decreases when passing from tension to shear, and the softening rates decreases when increasing the Lode parameter. Gao et al. [2009] performed both experimental tests and micro-mechanics analyses in

[3]Obtained by rotating an ellipse about one of its principal axes.

[4]Defined as the ratio between the diameter in the longitudinal direction and the diameter in the transverse direction.

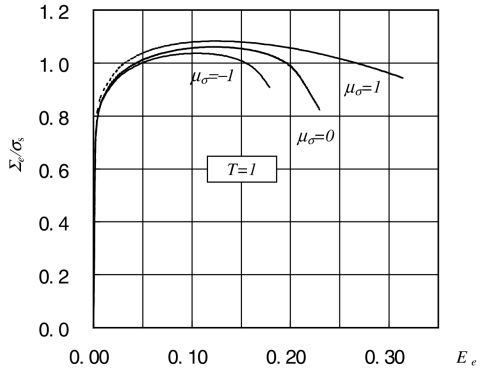

Figure 1: Equivalent stress-strain curves for different values of the Lode parameter [Zhang et al., 2001]. If the triaxiality is kept constant, the load carrying capacity diminish proportional to the Lode parameter.

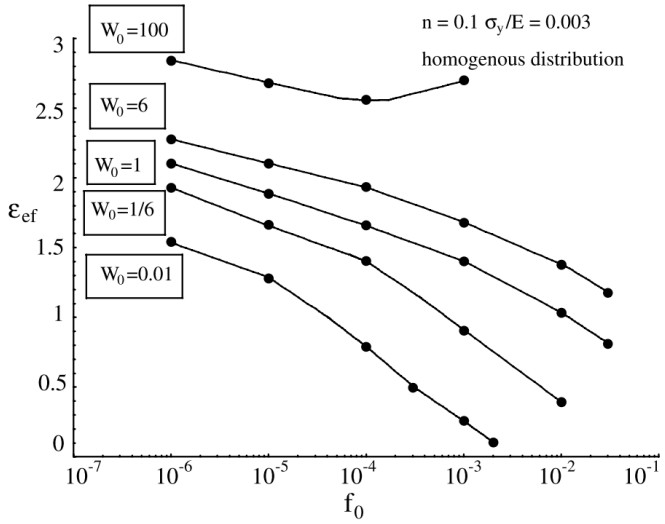

Figure 2: Influence of the void aspect ratio in the ductility of an ideal material [Pardoen, 2006].

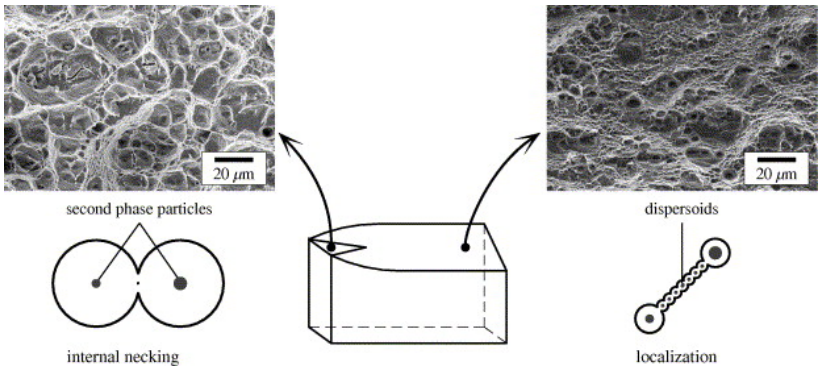

Figure 3: Two coalescence mechanisms [Bron and Besson, 2006]. The internal necking of voids is dominant at high values of triaxiality, while the second, characterised as a second population of voids (dispersoids or secondary dimples) that appeared between the primary voids, is dominant at low values.

order to demonstrate that the Lode angle has an important effect on ductile fracture. Considering a representative material volume (RMV) of a ficticious material, using J_2 plasticity within an updated lagrangian scheme in ABAQUS. Prescribed boundary conditions are imposed to keep both the triaxiality or the Lode angle constant (similar as in Zhang et al. [2001]). Failure is assumed to happen when localization of plastic flow takes place in the inter-void ligament [Koplik and Needleman, 1988] (uniaxial straining mode). It is shown in Fig. 5 that the Lode has an important effect the strain at coalescence. It is also shown in Fig. 6 that the effect of the Lode angle is lower at high triaxialities, coinciding with the results from Zhang et al. [2001]. Gao et al. [2009] also studied the effect of the secondary voids nucleation (Fig. 5 and Fig. 6, which reduce notable the ductility of the material.

[Nahshon and Hutchinson, 2008] extended the Gurson model to shear-dominated deformations by using the Lode parameter (see Eq. 1), in order to discriminate between axisymmetric and pure shear stress states. The incapability of the previous extended models (Leblond, Pardoen) are mainly based on solutions for voids subject to axisymmetric stressing and do not address the damage induced softening. The main idea was considered the void distorsion and inter-void interaction in a different the main factor detonating the softening and localization.

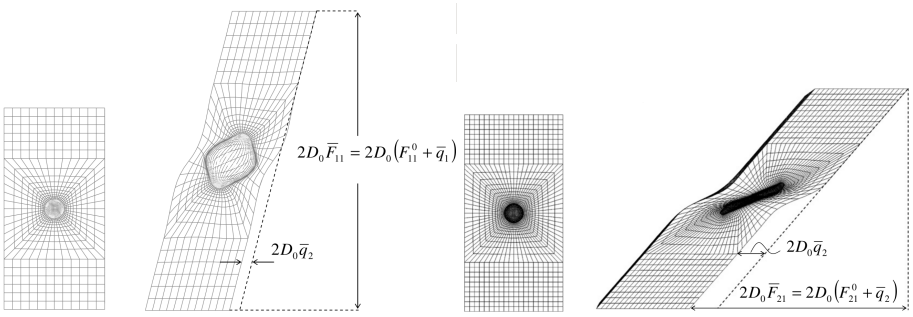

(a) Internal necking ($\beta = -0.85$, $T = 1.0$). (b) Shear localization ($\beta = -0.15$, $T = 0.5$).

Figure 4: Void coalescence mechanisms under different values of triaxiality and the Lode parameter [Barsoum and Faleskog, 2007a].

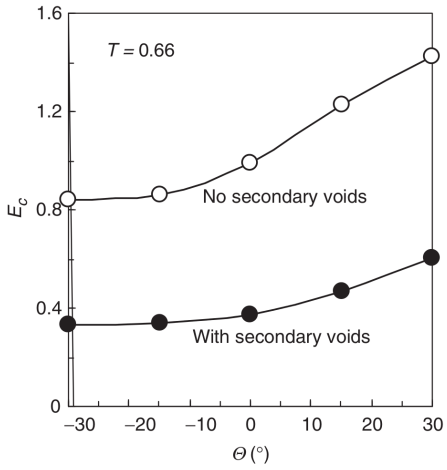

Figure 5: Effect of secondary voids and the Lode angle [Gao et al., 2009]. Triaxiality is kept constant at $T = 2/3$.

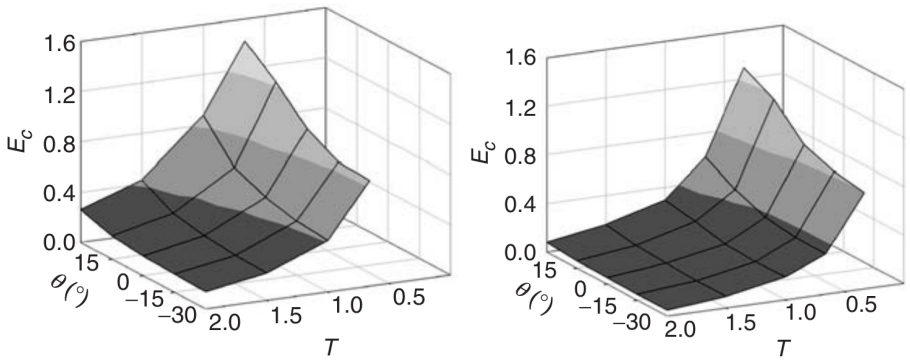

(a) Without secondary voids.

(b) With secondary voids.

Figure 6: Strain at localization E_c as a function of the triaxiality T and the Lode angle θ [Gao et al., 2009].

4 Experimental characterization

As mentioned in section 3, the effect of the Lode parameter becames prominent at low values of triaxiality. Hence, any experimental study about the influence of this parameter on ductile fracture should be carry on at low values of triaxiality. Traditionally, notched specimens are used to get different values of triaxiality and most of the advances in the area have been done using axisymmetric bar specimens. This was mainly motivated mainly due to computational reasons, as the simulations are faster using this hypothesis.

The drawback of using this kind of specimens is that they cannot reach values under $T = 1/3$ (limited by the theoretical value in a smooth tensile test specimen), and they also are subjected to axisymmetric stresses. Upsetting test could be use if bulk material is available, which is not possible if sheet metal is available.

In this section, different specimens used in the study of low triaxiality values are presented and described. This is by no means limited to the study of the Lode parameter, but for low-triaxiality range as a general experimental framework. Only sheet metal specimens are presented.

Gao et al. [2009] campaign. Gao et al. [2009] studied the influence of the Lode angle conducting test in several specimens, in order to ensure that failure occurs at different stress states. The specimens included smooth and round bars, plane strain specimens, plane stress specimens, Lindholm-type torsion specimen [Lindholm et al., 1980] and modified plane stress/strain specimens containing holes. Despite reaching a wide range of triaxialities (as T varies with the notch radius), the specimens only allows to get discrete values of the Lode parameter ($X = 1$ for and $X = 0$ for the torsion specimens and the circular-notched plane strain specimens).

Tension-torsion specimen To objective Barsoum and Faleskog [2007b] was gain understanding of the change of the ductile behaviour by analyzing the stress triaxiality, the Lode parameter and the effective plastic strain. In particular, the transition between low and high triaxiality rupture (coalescence) mechanism. To do this, a specially circumferentially double notched tube specimen subjected to a combination of tensile and torsional loading, was designed (Fig. 7). By changing the relation between the normal stress and the stress stress over the cross section, the triaxiality can be controlled.

It is important to note the dimensions used by the authors in Fig. 7, with a total height H of 120 mm, notch height h of only 1 mm and thickness $2t$

of 3.2 mm. Hence, this specimen should be carefully machined and aligned into the setup hardware.

Modified shear specimen Driemeier et al. [2010] studied the combined effect pf the stress intensity, triaxiality and lode parameter in the behavior of Al alloys. An experimental campaign was designed specifically to study the behavior of the material at low triaxialities. Flat tensile, notched and shear specimens, with two different thickness (1.56 mm and 6.35 mm) were tested. An Arcan [] of 6.35 mm specimen was also proposed to obtain information for different triaxialities. This specimen cannot be thinner because of instabilities due to torsional buckling. The shear specimens were slightly modified in order to investigate the effect of low values of triaxiality, introducing outplane notches between the central holes (Fig. 8). As the test for the thin sheets (1.56mm) do not show geometric effects, plane stress condi-

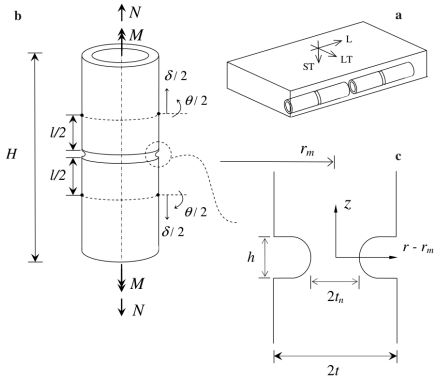

Figure 7: [Barsoum and Faleskog, 2007b].

Figure 8: Modified shear specimen with different lateral notches [Driemeier et al., 2010].

tions are assumed valid. Hence, the Lode angle cannot be studied because under this stress state, the Lode parameter is dependent on the triaxiality [Bai and Wierzbicki, 2008].

Butterfly specimen The butterfly specimen was initially planned to investigate the effect of different triaxiality levels on ductile fracture of thin sheet metals. The main characteristic is that the crack initiate in the center of the specimen, independently of the stress states being applied [Mohr and Henn, 2007]. In this way, addressing the experimental difficulty that fracture usually initializes in zones where the strain state is strongly heterogeneous. Moreover, the specimen can be charged in two different axis, allowing the onset of fracture to appear within different stress states, ranging from pure shear to transverse plane strain tension. An improved version of the specimen (adding a second curvature) was later used by Bai and Wierzbicki [2008] to calibrate a fracture locus sensible to the third invariant. Finally, Dunand and Mohr [2011b] improved the specimen geometry of [Mohr and Henn, 2007] to cover a wider range of stress states and different loading paths to fracture. Nevertheless, the complex geometry of the specimen is prone to initial imperfections. For instance, the last improved version from Dunand and Mohr [2011b] suffers from extreme sensibility to the cutting method which can easily leads to different results. As mentioned by Dunand and Mohr [2011b], local variations of the thickness should not be greater than 10 µm.

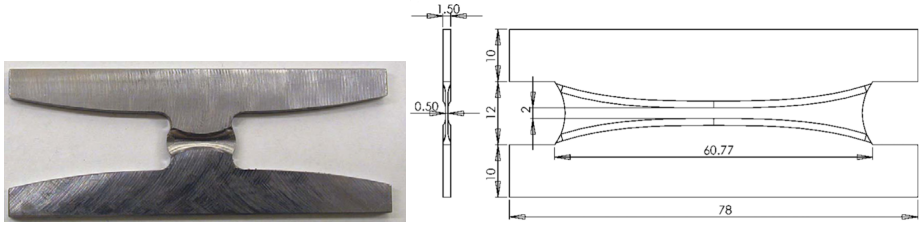

(a) Bai and Wierzbicki [2008]. (b) Dunand and Mohr [2011b].

Figure 9: Butterfly specimen evolution.

A Trigonometric remarks

The inverse trigonometric functions are multivalued functions. That is, a so called *function* that assume two or more distinct values in its range for at least one point in its domain. For instance, multiple values of w such that $z = \sin w$ so $\arccos z$ is not uniquely defined.

The problem with equation 18 is that the values of the right side of the equation (RSE) are sometimes greater than 1, which is impossible since the range of the cosine function is $-1 \leq \cos x \leq 1$. This leads to imaginary angles.

References

Y. Bai and T. Wierzbicki. A new model of metal plasticity and fracture with pressure and Lode dependence. *International Journal of Plasticity*, 24(6):1071–1096, June 2008. ISSN 07496419. doi: 10.1016/j.ijplas.2007.09.004. URL http://linkinghub.elsevier.com/retrieve/pii/S0749641907001246.

Y. Bai and T. Wierzbicki. Application of extended Mohr-Coulomb criterion to ductile fracture. *International Journal of Fracture*, 161(1):1–20, Nov. 2009. ISSN 0376-9429. doi: 10.1007/s10704-009-9422-8. URL http://www.springerlink.com/index/10.1007/s10704-009-9422-8.

J. P. Bardet. Lode Dependences for Isotropic Pressure-Sensitive Elastoplastic Materials. *Journal of Applied Mechanics*, 57(3):498, 1990. ISSN 00218936. doi: 10.1115/1.2897051. URL http://link.aip.org/link/JAMCAV/v57/i3/p498/s1&Agg=doi.

I. Barsoum and J. Faleskog. Rupture mechanisms in combined tension and shear-Micromechanics. *International Journal of Solids and Structures*, 44(17):5481–5498, Aug. 2007a. ISSN 00207683. doi: 10.1016/j.ijsolstr.2007.01.010. URL http://linkinghub.elsevier.com/retrieve/pii/S0020768306003921.

I. Barsoum and J. Faleskog. Rupture mechanisms in combined tension and shear-Experiments. *International Journal of Solids and Structures*, 44(6):1768–1786, Mar. 2007b. ISSN 00207683. doi: 10.1016/j.ijsolstr.2006.09.031. URL http://linkinghub.elsevier.com/retrieve/pii/S0020768306003921.

A. M. Beese and D. Mohr. Anisotropic plasticity model coupled with Lode angle dependent strain-induced transformation kinetics law. *Journal of the Mechanics and Physics of Solids*, 60(11):1922–1940, Nov. 2012. ISSN 00225096. doi: 10.1016/j.jmps.2012.06.009. URL http://linkinghub.elsevier.com/retrieve/pii/S0022509612001299.

F. Bron and J. Besson. Simulation of the ductile tearing for two grades of 2024 aluminum alloy thin sheets. *Engineering Fracture Mechanics*, 73(11):1531–1552, July 2006. ISSN 00137944. doi: 10.1016/j.engfracmech.2006.01.024. URL http://linkinghub.elsevier.com/retrieve/pii/S0013794406000646.

M. Brünig, S. Berger, and H. Obrecht. Numerical simulation of the localization behavior of hydrostatic-stress-sensitive metals. *International Journal of Mechanical Sciences*, 42(11):2147–2166, Nov. 2000. ISSN 00207403. doi: 10.1016/S0020-7403(00)00002-3. URL http://linkinghub.elsevier.com/retrieve/pii/S0020740300000023.

T. Coppola, L. Cortese, and P. Folgarait. The effect of stress invariants on ductile fracture limit in steels. *Engineering Fracture Mechanics*, 76(9):1288–1302, June 2009. ISSN 00137944. doi: 10.1016/j.engfracmech.2009.02.006. URL http://linkinghub.elsevier.com/retrieve/pii/S0013794409000459.

K. Danas and P. Ponte Castañeda. Influence of the Lode parameter and the stress triaxiality on the failure of elasto-plastic porous materials. *International Journal of Solids and Structures*, 49(11-12):1325–1342, June 2012. ISSN 00207683. doi: 10.1016/j.ijsolstr.2012.02.006. URL http://linkinghub.elsevier.com/retrieve/pii/S0020768312000467.

L. Driemeier, M. Brünig, G. Micheli, and M. Alves. Experiments on stress-triaxiality dependence of material behavior of aluminum alloys. *Mechanics of Materials*, 42(2):207–217, Feb. 2010. ISSN 01676636. doi: 10.1016/j.mechmat.2009.11.012. URL http://linkinghub.elsevier.com/retrieve/pii/S0167663609001999.

D. Drucker and W. Prager. Soil Mechanics and Plastic Analysis or Limit Design. *Quarterly of Applied Mathematics*, 10(2):157–165, 1952.

M. Dunand and D. Mohr. On the predictive capabilities of the shear modified Gurson and the modified Mohr-Coulomb fracture models over a wide range of stress triaxialities and Lode angles. *Journal of the Mechanics and Physics of Solids*, 59(7):1374–1394, July 2011a. ISSN 00225096. doi: 10.1016/j.jmps.2011.04.006. URL http://linkinghub.elsevier.com/retrieve/pii/S0022509611000688.

M. Dunand and D. Mohr. Optimized butterfly specimen for the fracture testing of sheet materials under combined normal and shear loading. *Engineering Fracture Mechanics*, 78(17):2919–2934, Dec. 2011b. ISSN 00137944. doi: 10.1016/j.engfracmech.2011.08.008. URL http://linkinghub.elsevier.com/retrieve/pii/S0013794411003067.

X. Gao, G. Zhang, and C. Roe. A Study on the Effect of the Stress State on Ductile Fracture. *International Journal of Damage Mechanics*, 19(1):75–94, June 2009. ISSN 1056-7895. doi: 10.1177/1056789509101917. URL http://ijd.sagepub.com/cgi/doi/10.1177/1056789509101917.

M. Gologanu, J.-B. Leblond, G. Perrin, and J. Devaux. Recent extensions of Gurson's model for porous ductile materials. *International Seminar of Micromechanics*, pages 61–130, 1996.

A. Gurson. Continuum theory of ductile rupture by void nucleation and growth: Part I-Yield criteria and flow rules for porous ductile media. *Journal of Engineering Materials and Technology*, 99(1):2–15, 1977.

A. Khan and S. Huang. *Continuum theory of plasticity*. 1995. ISBN 978-0471310433.

J. Koplik and A. Needleman. Void growth and coalescence in porous plastic solids. *International Journal of Solids and Structures*, 24(8):835–853, Jan. 1988. ISSN 00207683. doi: 10.1016/0020-7683(88)90051-0. URL http://linkinghub.elsevier.com/retrieve/pii/0020768388900510.

D. Lassance, D. Fabregue, F. Delannay, and T. Pardoen. Micromechanics of room and high temperature fracture in 6xxx Al alloys. *Progress in Materials Science*, 52(1):62–129, Jan. 2007. ISSN 00796425. doi: 10.1016/j.pmatsci.2006.06.001. URL http://linkinghub.elsevier.com/retrieve/pii/S0079642506000399.

H. Li, M. Fu, J. Lu, and H. Yang. Ductile fracture: Experiments and computations. *International Journal of Plasticity*, 27(2):147–180, Feb. 2011. ISSN 07496419. doi: 10.1016/j.ijplas.2010.04.001. URL http://linkinghub.elsevier.com/retrieve/pii/S0749641910000598.

U. S. Lindholm, A. Nagy, G. R. Johnson, and J. M. Hoegfeldt. Large strain, high strain rate testing of copper. *Journal of engineering materials and technology*, 102:376, 1980.

W. Lode. Versuche über den Einflußder mittleren Hauptspannung auf das Fließen der Metalle Eisen, Kupfer und Nickel. *Zeitschrift für Physik*, 36(11-12):913–939, Nov. 1926. ISSN 1434-6001. doi: 10.1007/BF01400222. URL http://www.springerlink.com/index/10.1007/BF01400222.

L. Malcher, F. Andrade Pires, and J. César de Sá. An assessment of isotropic constitutive models for ductile fracture under high and low stress triaxiality. *International Journal of Plasticity*, 30-31:81–115, Mar. 2012. ISSN 07496419. doi: 10.1016/j.ijplas.2011.10.005. URL http://linkinghub.elsevier.com/retrieve/pii/S0749641911001690.

D. Mohr and S. Henn. Calibration of Stress-triaxiality Dependent Crack Formation Criteria: A New Hybrid Experimental-Numerical Method. *Experimental Mechanics*, 47(6):805–820, Feb. 2007. ISSN 0014-4851. doi: 10.1007/s11340-007-9039-7. URL http://link.springer.com/10.1007/s11340-007-9039-7.

T. Morgeneyer and J. Besson. Flat to slant ductile fracture transition: Tomography examination and simulations using shear-controlled void nucleation. *Scripta Materialia*, 65(11):1002–1005, Dec. 2011. ISSN 13596462. doi: 10.1016/j.scriptamat.2011.09.004. URL http://linkinghub.elsevier.com/retrieve/pii/S1359646211005306.

K. Nahshon and J. Hutchinson. Modification of the Gurson Model for shear failure. *European Journal of Mechanics - A/Solids*, 27(1):1–17, Jan. 2008. ISSN 09977538. doi: 10.1016/j.euromechsol.2007.08.002. URL http://linkinghub.elsevier.com/retrieve/pii/S0997753807000721.

T. Pardoen. Numerical simulation of low stress triaxiality ductile fracture. *Computers & Structures*, 84(26-27):1641–1650, Oct. 2006. ISSN 00457949. doi: 10.1016/j.compstruc.2006.05.001. URL http://linkinghub.elsevier.com/retrieve/pii/S0045794906001659.

T. Pardoen and Y. Brechet. Influence of microstructure-driven strain localization on the ductile fracture of metallic alloys. *Philosophical Magazine*, 84(3-5):269–297, Jan. 2004. ISSN 1478-6435. doi: 10.1080/14786430310001610366. URL http://www.tandfonline.com/doi/abs/10.1080/14786430310001610366.

V. Tvergaard and A. Needleman. Analysis of the cup-cone fracture in a round tensile bar. *Acta Metallurgica*, 32(1):157–169, Jan. 1984. ISSN 00016160. doi: 10.1016/0001-6160(84)90213-X. URL http://linkinghub.elsevier.com/retrieve/pii/000161608490213X.

G. Z. Voyiadjis, S. Hoseini, and G. Farrahi. Effects of stress invariants and reverse loading on ductile fracture initiation. *International Journal of Solids and Structures*, 49(13):1541–1556, June 2012. ISSN 00207683. doi: 10.1016/j.ijsolstr.2012.02.030. URL http://linkinghub.elsevier.com/retrieve/pii/S0020768312000789.

T. Wierzbicki, Y. Bao, Y.-W. Lee, and Y. Bai. Calibration and evaluation of seven fracture models. *International Journal of Mechanical Sciences*, 47(4-5):719–743, Apr. 2005. ISSN 00207403. doi: 10.1016/j.ijmecsci.2005.03.003. URL http://linkinghub.elsevier.com/retrieve/pii/S0020740305000822.

K. Zhang, J. Bai, and D. François. Numerical analysis of the influence of the Lode parameter on void growth. *International Journal of Solids and Structures*, 38(32-33):5847–5856, Aug. 2001. ISSN 00207683. doi: 10.1016/S0020-7683(00)00391-7. URL http://www.sciencedirect.com/science/article/pii/S0020768300003917http://linkinghub.elsevier.com/retrieve/pii/S0020768300003917.